The relationship between the Madden Julian Oscillation and the North Atlantic Oscillation

Zhina Jiang

State Key Laboratory of Severe Weather (LaSW), Chinese Academy of Meteorological Sciences, Beijing, China

Steven B. Feldstein

Department of Meteorology, The Pennsylvania State University, University Park, Pennsylvania, USA

Sukyoung Lee

Department of Meteorology, The Pennsylvania State University, University Park, Pennsylvania, USA; School of Earth and Environmental Sciences, Seoul National University, Seoul, South Korea

Corresponding author address: Zhina Jiang, State Key Laboratory of Severe Weather (LaSW), Chinese Academy of Meteorological Sciences, No.46, Zhongguancun South Road, Haidian District, Beijing 100081, China

Email: jzn@camscma.cn

August 1, 2016

Abstract

In this study, the relationship between the Madden-Julian Oscillation (MJO) and the North Atlantic Oscillation (NAO) is investigated by analyzing NAO events both when the MJO is active and inactive. The European Centre for Medium-Range Weather Forecasts Re-analysis (ERA-Interim) dataset is used, for the years 1979-2006 and the months of December-February.

When the MJO is active, negative (positive) NAO events are preceded by enhanced MJO convection over the tropical western and central Pacific Ocean (tropical Indian Ocean and Maritime Continent). The accompanying sea level pressure (SLP) anomaly fields reveal patterns that closely resemble the Northern Annular Mode (NAM). The MJO-related negative NAO events are preceded by an increase in the vertical propagation of planetary-scale wave activity into the stratosphere, followed by a marked weakening of the zonally-symmetric component of the lower stratospheric zonal wind. The opposite behaviour is found for the MJO-related positive NAO events. The MJO-related NAO events are also long-lived, persisting for approximately 30 days. In contrast, when the MJO is inactive, there is little change to the zonally-symmetric component of the lower stratospheric zonal wind, these events are relatively short-lived, lasting for about 10 days, and the NAO corresponds to

dipole that is confined to the North Atlantic.

Key words: Madden-Julian Oscillation, North Atlantic Oscillation, Northern Annular Mode

1. Introduction

The North Atlantic Oscillation (NAO) is one of the dominant modes of Northern Hemisphere winter climate variability. The NAO takes on the form of a north-south dipole in the North Atlantic sea level pressure field (Walker and Bliss, 1932; Hurrell, 1995; Hurrell and Loon, 1997), and has a time scale that ranges from several days to weeks (Feldstein, 2000, 2003; Benedict et al., 2004; Franzke et al., 2004; Luo et al., 2007; Jiang et al., 2013). Although the NAO amplitude time series can be approximated by a first-order autoregressive process with a 7-10 day *e*-folding time scale (Feldstein, 2000, 2003), nowadays there are numerical models that can predict the NAO in the medium and extended range, that is, from one to four weeks (e.g., Vitart and Molteni, 2010).

Several observational studies have also found that there is an extended-range linkage between the frequency of occurrence of the NAO and the phase (Wheeler and Hendon 2004) of the intraseasonal time scale Madden-Julian Oscillation (MJO) (e.g., Cassou, 2008; Lin et al., 2009, 2010; Riddle et al., 2013). (The representation of the MJO with indices that measure its amplitude and phase is described in sections 2 and

3.) The MJO is the dominant mode of intraseasonal (30–90 days) variability in the tropical atmosphere, and is characterized by a planetary-scale (zonal wavenumbers 1-3) convectively coupled circulation field (Madden and Julian, 1971, 1994). Cassou (2008) provided evidence that phases 3 and 6 of the MJO are precursors with lead times of up to 14 days of the positive and negative NAO phases, respectively, where phase 3 (phase 6) corresponds to MJO convection in the tropical Indian (western Pacific) Ocean. Consistent findings have also been presented by Lin et al. (2009). These statistical studies find that an active MJO is followed several weeks later by an increase in the frequency of occurrence of either NAO phase by as much as 70%. Similarly, Zhou and Miller (2005) demonstrated that when MJO convection is enhanced (diminished) over the Indian Ocean, the Arctic Oscillation (AO, also referred to as the Northern Annular Mode (NAM) (Thompson and Wallace, 1998; 2000)), which closely resembles the NAO except for the presence of a third centre of action over the North Pacific, tends to favour its high (low) index polarity, with a time lag of up to 30 days.

These studies lead to the question of what is the mechanism through which the MJO influences the NAO. One possibility is simply that tropical convection excites Rossby waves that propagate poleward through the troposphere toward the North Atlantic where both NAO phases are excited via wave breaking (Benedict et al., 2004; Franzke et al., 2004). Another possible pathway involves the stratosphere, whereby

poleward propagating Rossby waves, excited by tropical convection, interfere with the climatological stationary eddies. This alters the vertical propagation of planetary-scale wave activity into the stratosphere, which changes the strength of the stratospheric polar vortex, and subsequently impacts the NAM in the troposphere, and thus also the NAO. Such a pathway was observed by Garfinkel et al. (2012) during sudden stratospheric warming events.

Even though the linkage between the MJO and NAO is well established, there remains the question of whether some NAO events are not related to the MJO or to other forms of tropical convection. The possibility that some NAO events may not be related to tropical convection is suggested by the results of many idealized model studies which show that zonal index[1] fluctuations take place in the absence of tropical convection. (In the atmosphere, the zonal index is highly correlated with the NAO (DeWeaver and Nigam, 2000)). For example, zonal index fluctuations are found in barotropic models (e. g., Vallis et al., 2004), two-layer models (e.g., Robinson, 1991; Lee and Feldstein, 1996), and multi-level primitive equation models (e.g., Feldstein and Lee, 1996; Lorenz and Hartmann, 2001, 2003).

In this study, to explore the dynamical relationship between the MJO and NAO,

[1] The zonal index was originally defined by Rossby (1939) as a measure of the strength of the midlatitude zonal-mean zonal wind. Later studies, such as Robinson (1991), Yu and Hartmann (1993), and Feldstein and Lee (1996), define the zonal index in terms of empirical orthogonal functions of the zonal-mean zonal wind or relative angular momentum.

and also the dynamical processes that drive NAO events that are independent of the MJO, we divide NAO events into two categories; for one category, the NAO events are chosen to be preceded by specific phases of an active MJO (Zhou and Miller, 2005; Cassou, 2008; Lin et al., 2009) and the other category corresponds to NAO events that are unrelated to the MJO. We then explore the physical mechanisms that drive these two types of NAO events.

The outline of this paper is as follows. In section 2, the data and methodology are presented. This is followed in section 3 by an examination of the composite evolution of both types of NAO events, and the impact of tropical convection on the onset of NAO. The relationship between the two categories of NAO events and the NAM in the troposphere and stratosphere is presented in section 4. The conclusions are presented in section 5.

2. Data and methodology

a. Data

In this study, we utilize the daily (00Z) European Centre for Medium-Range Weather Forecasts (ECMWF) ERA-Interim Reanalysis sea level pressure (SLP), wind, and relative vorticity data (Dee et al., 2011). The corresponding streamfunction field is determined from the relative vorticity. Our focus is on the boreal winter for the months of December-February (DJF) for the period of 1979 to 2006.

Interpolated daily average, National Oceanic and Atmospheric Administration (NOAA) outgoing long wave radiation (OLR) data (Liebmann and Smith, 1996) is used to investigate deep convection in the tropics associated with the NAO. To represent the MJO, the Real-Time Multivariate MJO (RMM) index of Wheeler and Hendon (2004) is used. This index is based on a pair of combined empirical orthogonal functions (EOFs) of the near-equatorially-averaged 850-hPa zonal wind, 200-hPa zonal wind, and OLR fields. The projection of the daily observed data onto the multiple-variable EOFs, with the annual cycle and interannual variability removed, yields the Real-time Multivariate MJO times series 1 (RMM1), and MJO time series 2 (RMM2), which correspond to the principal component time series of the first two combined EOFs. Wheeler and Hendon (2004) defined the amplitude of the MJO to be the square root of the sum of RMM1 squared and RMM2 squared. The daily values of RMM1 and RMM2 are obtained from the Australian Bureau of Meteorology.

As discussed in the Introduction, we investigate whether the stratospheric polar vortex plays a role in the linkage between the MJO and NAO. To quantity the state of the stratospheric polar vortex, we use the NAM indices of Baldwin and Dunkerton (1999), defined as the leading EOF at 17 different pressure levels of the 90-day low-pass-filtered geopotential north of 20°N. This cutoff period is appropriate for the present study, since a 90-day cycle has an *e*-folding time scale of a little less than one-quarter of the cycle, i.e., less than 22.5 days. As is shown in Gerber et al. (2010;

Fig. 8 of that paper), in the stratosphere, the *e*-folding time scale for the NAM during the winter season for ERA-40 Reanalysis data varies from 25 to 30 days. The daily NAM indices can be downloaded from http://people.nwra.com/resumes/baldwin/nam_index_1958-2006.txt.

b. Selection criteria of NAO events

To identify the NAO spatial pattern, an EOF analysis of the daily ECMWF ERA-Interim SLP field is performed for the North Atlantic Ocean restricted to the domain between 25^{o}N and 80^{o}N and between 70^{o}W and 40^{o}E. Anomalies are calculated by subtracting the seasonal cycle at each grid point, which is represented by the first two harmonics of the calendar-day mean annual cycle. The NAO corresponds to the first EOF and contributes toward 21.0% of the fractional variance (see Fig. 1). A typical NAO dipole is seen, with a positive anomaly spread across the mid-latitude North Atlantic, and a negative anomaly centred over Iceland.

NAO events are defined based on the application of a set of criteria on the principal component time series of the NAO (denoted as the NAO index). First, a string of three or more consecutive days with the amplitude of the NAO index being greater than one standard deviation is chosen as a "candidate". If the time interval of two consecutive candidates is less than 4 days, the latter candidate is not considered. The "lag 0 day", referred to as the onset day, is defined as the first day on which the NAO

index exceeds the one standard deviation threshold. This analysis is limited to events that take place within the DJF winter period, although a few days in November and March are sometimes included for compositing days that occur either before, or after, an event. This selection procedure yields 24 negative and 31 positive NAO events during the winter season from 1979 to 2006. Based on the onset days of these NAO events, we calculate lagged composites of key atmospheric variables associated with the excitation of the NAO events.

c. MJO- and non-MJO NAO events

To identify the state of the MJO prior to the NAO events, we divide the days from lag -15 to lag -6 into two pentads. For the positive NAO (NAO+ hereafter), if the mean amplitude of the MJO index for either of these two pentads is larger than 1.3[2], then the NAO+ event is considered to be an MJO-related NAO+ event. (The findings of this study were found to be relatively insensitive to the threshold value chosen for both positive and negative NAO events.) For the sake of brevity, these events will be referred to as NAO+|MJO events, where the pipe symbol (|) is used to indicate that the NAO+ event is preceded by an active MJO. If the mean amplitude of the MJO index for both of these two pentads is less than 1.3, then the NAO+ event is

[2]This value of 1.3 corresponds to the peak in the probability density function (PDF) of the MJO amplitude (not shown).

considered as a non-MJO NAO+ event. For brevity, these events will be denoted as NAO+|nMJO events. Furthermore, since MJO phases 2, 3, 4 (enhanced convection over the Indian Ocean and the Maritime Continent) are most likely to be followed by NAO+ events (Zhou and Miller, 2005; Cassou, 2008; Lin et al., 2009), the NAO+|MJO events are further divided into NAO+|MJO (2, 3, 4) events and NAO+|MJO (1, 5, 6, 7, 8) events. For the negative NAO (NAO- hereafter), an analogous definition of NAO-|MJO events and NAO-|nMJO events is applied, except for the threshold MJO amplitude being 1.4. Similarly, since MJO phases 6, 7, 8 (increased convection over the western and central tropical Pacific Ocean) occur most frequently prior to NAO- events, the NAO-|MJO events are divided into NAO-|MJO (6, 7, 8) events and NAO-MJO (1, 2, 3, 4, 5) events. For both NAO phases, we will not consider the NAO+|MJO (1, 5, 6, 7, 8) and NAO-|MJO (1, 2, 3, 4, 5) events. Following this definition, there are 15 NAO+|MJO (2, 3, 4) events, 12 NAO+|nMJO events, 10 NAO-|MJO (6, 7, 8) events, and 8 NAO-|nMJO events. Therefore, according to this definition, slightly more than 50% of the NAO events are associated with the MJO. For brevity, the NAO+|MJO (2, 3, 4) events will be referred to as NAO+|MJO events, and the NAO-|MJO (6, 7, 8) events will be referred to as NAO-|MJO events.

A two-sided Student's *t*-test and Monte Carlo bootstrapping are used to evaluate the statistical significance of our composite calculations. We briefly describe the Monte

Carlo bootstrapping. Firstly, if there are *n* events that comprise a composite, then we randomly choose *n* onset days and calculate lagged composite values in the same manner as that for the onset days associated with the NAO events. We repeat this calculation 1000 times, which will yield a distribution of 1000 random lagged composite values at each grid point. We then compare the lagged composite values from the NAO events to the distribution of 1000 random values. If the NAO composite value falls within the top 50 or bottom 50 values, then the lagged composite value is regarded as statistically significant at the 90% confidence level.

3. Intraseasonal characteristics of the composite NAO evolution

In this section, we examine the composite life cycles of the NAO|MJO and NAO|nMJO events. Lagged composites of the NAO index, relative to the onset day, are shown in Fig. 2. For both phases, the NAO index has a small amplitude at lag -4 days. For both types of NAO- events, the NAO index reaches its maximum amplitude at lag +2 days, and by lag +15 days it has decayed to a relatively small value. Similar behaviour is seen for both types of NAO+ events, except for the NAO index being of opposite sign and attaining its maximum amplitude at lag +1 days. In conclusion, it takes about two weeks for the NAO to complete its life cycle, which is consistent with the results of Feldstein (2003). In addition, for both NAO phases, the composite evolution of the NAO index for both the NAO|MJO and NAO|nMJO events are rather

similar.

To verify that our definition of NAO|MJO and NAO|nMJO events adequately distinguishes between an active and inactive MJO, and to evaluate the relationship between the various NAO events and the MJO phase, we calculate composites of the MJO amplitude, RMM1, and RMM2 at lags extending back to lag -50 days. The results are shown in Fig. 3. For the NAO-|MJO events (Fig. 3a), the MJO amplitude is largest between lag -25 and lag -5 days, with values greater than 1.6, well in excess of its climatological mean value of 1.2. From lag -50 to lag -40 days the MJO is in phases 2 and 3, from lag -21 to lag -13 days, the MJO is in phases 5 and 6, and from lag -13 to lag -1 days, the MJO is in phases 7 and 8. (To visualize the location of the anomalous convection associated with the MJO, we reproduce Fig. 8 of Wheeler and Hendon (2004) which shows the OLR anomalies for all 8 phases of the MJO (see Fig. 4).) For the NAO-|nMJO events (Fig. 3b), the MJO amplitude remains close to its climatological value throughout the negative lags, and it exhibits an increase in value beginning at about lag +10 days.

It is seen for the NAO+|MJO events (Fig. 3c) that the MJO amplitude exceeds a value of 1.6 between lag -20 days and lag -5 days. From lag -50 to lag -30 days the MJO is in phases 8 and 1, from lag -25 to lag -14 days the MJO is in phases 1 and 2, and from lag -14 to lag -2 days the MJO is in phases 3 and 4 (Fig. 3c). For the NAO+|nMJO events (Fig. 3d), prior to about lag -5 days, the MJO amplitude remains

small, well below its climatological mean value.

To further illustrate the relationship between tropical convection and the NAO development, we show the composite anomalous OLR field for the time interval from lag -15 to lag -1 days relative to the NAO onset. In this calculation, this time period is divided into three separate pentads: lag -3 pentads (averaged from lag −15 to −11 days), lag -2 pentads (averaged from lag -10 to -6 days) and lag -1 pentads (averaged from lag -5 to -1 days). Since the tropical OLR field is dominated by planetary waves, the OLR field is truncated to zonal wavenumbers less than and equal to 4.

Figure 5 shows the composite anomalous planetary-scale OLR fields for the NAO events. Shaded areas indicate statistical significance above the 90% confidence level according to a two-sided Student's *t*-test. As can be seen in Fig. 5a, the NAO-|MJO events are preceded by a significant reduction in convection (positive OLR anomalies) over the tropical Indian Ocean and increased convection (negative OLR anomalies) over the western and central tropical Pacific Ocean at all three pentads, which correspond to MJO phases 6, 7, and 8, and is consistent with the findings of previous studies that relate the MJO to the NAO (Zhou and Miller 2005; Cassou 2008; Lin et al. 2009). For the NAO-|nMJO events, shown in Fig. 5b, compared to the NAO-|MJO events, the convective activity associated with the NAO-|nMJO is much weaker, and shows statistical significance over a much smaller area.

The NAO+|MJO events are found to have a stronger OLR signal than the

NAO+|nMJO events for all three pentads (Figs. 5c and 5d). As can be seen from Fig. 5c, the NAO+|MJO events are associated with increased convection over the tropical Indian Ocean and reduced convection over the Maritime Continent, being most evident for the first two pentads. The anomalous OLR field corresponds to MJO phases 2, 3, and 4. This MJO/NAO+ phase relationship is again consistent with the results of previous studies (Zhou and Miller 2005; Cassou 2008; Lin et al. 2009).

The composite evolution of the anomalous SLP field for the NAO- events is shown in Fig. 6. For the NAO-|MJO events (Fig. 6a), it is seen that two positive anomalies at lag -5 days, one located to the east of Greenland, and the other over northwestern Siberia, merge by lag 0 days, resulting in the development of a high-over-low dipole anomaly. This dipole anomaly then moves westward toward Greenland and the North Atlantic, and forms the negative phase NAO. The NAO- persists through to lag +10 days. Also, at each lag from lag -10 to lag +10 days, and for the lag -10 to lag +10 day time average, one can see a statistically significant negative SLP anomaly over the northeast Pacific at a similar latitude as that for the North Atlantic. Because of the presence of the negative SLP anomaly over the North Pacific, the hemispheric SLP anomaly pattern appears to more closely resemble the negative phase of the NAM (NAM- hereafter) rather that a localized NAO- dipole confined to the North Atlantic. For the NAO-|nMJO events (Fig. 6b), it is seen that a positive anomaly is present over western Siberia at lag -10 days, which propagates westward and forms the positive

anomaly of the NAO- dipole at lag 0 days. By lag +10 days, the NAO- anomalies have weakened. In contrast to the NAO-|MJO events, the lag -10 to lag +10 day time average anomaly pattern for the NAO-|nMJO events indicates the presence of a relatively weak positive anomaly over the North Pacific centred at a latitude that corresponds to the node of the North Atlantic dipole anomaly. In other words, the NAO-|nMJO events appear to closely resemble the localized NAO- and not the NAM-.

Figure 7 shows the composite anomalous SLP fields for NAO+ events. For the NAO+|MJO (Fig. 7a), it is seen that a low-over-high dipole NAO+ pattern forms by lag 0 days and persists until lag +10 days. In analogy with the NAO-|MJO events, over the midlatitude North Pacific, a statistically significant positive SLP anomaly is found from lag -10 to lag +10 days and in the lag -10 to lag +10 day time average. In addition, since the North Pacific and North Atlantic anomalies are centred at a similar latitude, the hemispheric SLP anomaly pattern resembles the positive NAM phase (NAM+ hereafter). For the NAO+|nMJO (Fig. 7b), a statistically significant NAO+ dipole also appears at lag 0 days. By lag +10 days, this NAO+ dipole has mostly decayed. Over the midlatitude North Pacific, a relatively weak negative anomaly can be found at most lags from lag -10 to lag +10 days, and also in the time average. As this anomaly is of opposite sign compared to that for the midlatitude North Atlantic, the NAO+|nMJO events appears to more closely resemble the NAO+

than the NAM+.

The above results suggest that the NAO|MJO events (for both phases) are associated with the NAM, rather than a localized NAO, because of the presence of the North Pacific SLP anomalies that are of the same sign as those over the North Atlantic. In contrast, the NAO|nMJO events (for both phases) are better described as corresponding to the NAO, because of the absence of similar signed North Pacific anomalies.

For both NAO phases, one feature of the extratropical response to the MJO, as discussed above, is that the largest amplitude anomalies occur over the North Atlantic. A plausible explanation for this behaviour involves the spatial structure of the background flow over the North Atlantic as well as the storm track eddies being strongest over the North Atlantic.

Before considering the role of the background flow and the amplitude of storm track eddies, it is helpful to first discuss the linkage between the stratospheric NAM and tropospheric NAM. As shown by Garfinkel et al. (2013), using a general circulation model, a change in the strength of the stratospheric polar vortex, i.e., the occurrence of a stratospheric NAM anomaly, coincides with the excitation of a tropospheric NAM anomaly that amplifies via a positive synoptic-scale eddy feedback in the troposphere. A widely accepted mechanism for the initial excitation of the tropospheric NAM by the stratospheric NAM involves the process of downward

control (Polvani and Kushner, 2002; Kushner and Polvani 2004; Song and Robinson 2004; Simpson et al., 2009).

Frankze et al. (2004) suggested that the North Atlantic is a region that is favored for the development of NAO-like anomalies because of the small meridional potential vorticity gradient of the background flow in the jet exit region. This is because large parcel displacements tend to occur in regions where the meridional potential vorticity gradient is small. Within the jet exit region, they showed that large amplitude synoptic-scale disturbances that are on the poleward side of the North Atlantic jet break cyclonically and evolve into the negative NAO. Analogously, they found that large amplitude synoptic-scale disturbances on the equatorward side of the jet break anticyclonically and develop into the positive NAO. Thus, the North Atlantic appears to be a region that is favourable for further amplification of NAO-like anomalies via a synoptic-scale eddy feedback.

Observations show that during the winter the storm track over the North Atlantic is stronger than that over the North Pacific. An explanation for these differences in storm track strength has been offered by Lee and Kim (2003). Their model findings suggest that storm track eddies are stronger over the midlatitude North Atlantic because of the relative strength of the subtropical jet over the two ocean basins. Over the North Pacific, the much stronger subtropical jet traps storm track eddies within that jet and suppresses the development of large amplitude eddies farther northward.

In contrast, because the subtropical jet is much weaker over the North Atlantic, the trapping of storm track eddies in the subtropical jet does not take place. Instead, a larger amplitude storm track develops over the midlatitude North Atlantic. Therefore, because storm track eddies are particularly strong over the North Atlantic, it is also expected that the North Atlantic is a preferred region for the amplification of NAO-like anomalies via a positive synoptic-scale eddy feedback.

4. Relationship to the NAM in the troposphere and stratosphere

In this section, we examine the relationship with the NAM in the troposphere and stratosphere during the various NAO events. Figure 8 shows the lagged composite NAM indices for the NAO- and NAO+ events, respectively. Two important points stand out in this figure. First, the NAM anomalies for the NAO|MJO events persist for much longer than those for the NAO|nMJO events (statistically significant NAM index anomalies persist for about 30 days in the NAO|MJO events and for about 10 days in the NAO|nMJO events). These NAM index anomalies extend through both the troposphere and stratosphere and are excited at about the same time. Second, there are large amplitude (statistically significant) NAM index anomalies in the stratosphere for the NAO|MJO events but not for the NAO|nMJO events. For the NAO-|MJO events (Fig. 8a), the occurrence of negative values of the NAM index in the stratosphere at negative lags days indicates that a weakened stratospheric polar vortex takes place

prior to the excitation of the NAO-|MJO events. Analogously, for the NAO+|MJO events (Fig. 8c), the positive NAM index values in the stratosphere indicate that these events are preceded by a strengthened stratospheric polar vortex.

We next examine the relationship between the phase of the MJO and the NAM index during the NAO|MJO events. First, the time interval from lag -40 to lag -25 days is considered. For the NAO-|MJO events, at lag -40 days, the MJO is located between phases 2 and 3, and at lag -25 days the MJO is in phase 4. These phases correspond to enhanced convection over different parts of the Indian Ocean. As shown by Zhou and Miller (2005) and Cassou (2008), enhanced convection in the Indian Ocean is followed by the positive phase of the AO and NAO, respectively, not the negative phase of the NAM, as in Fig. 8a. It is also important to note that over the lag -40 to lag -25 day time interval the MJO amplitude is small, close to its climatological value of 1.2, and the NAM index is not statistically significant. These results don't present sufficient support for a connection between the MJO and NAM over the lag -40 to lag -25 day time period.

If we consider later lags, a different picture emerges. For example, from lag -20 to lag -10 days, the MJO transitions from phase 5 to phase 7. Cassou (2008) showed that these MJO phases are followed by the negative NAO. Since Fig. 8a shows a negative NAM index in both the troposphere and stratosphere after lag -20 days, our results are consistent with those of Zhou and Miller (2005) and Cassou (2008). It should also be

noted that the MJO amplitude becomes large at about lag -20 days, and the NAM index first becomes statistically significant near this lag. This consistency with previous studies suggests that the MJO does drive the NAM during NAO-|MJO events, but only after lag -20 days.

A similar relationship for the NAO+|MJO events is also found (Fig. 8c), as the MJO phase and NAM index are consistent with Zhou and Miller (2005) and Cassou (2008) after lag -20 days, but not before. Furthermore, for the NAO+|MJO events, the MJO amplitude is also much smaller before lag -20 days, but the NAM index in the stratosphere is statistically significant from lag -40 to lag -20 days. However, over this time period the magnitude of the NAM index in the stratosphere is similar to that in the troposphere. These results also suggest that the MJO drives the NAM during NAO+|MJO events after lag -20 days.

Garfinkel et al. (2010, 2012) showed that the strength of the stratospheric polar vortex is altered through interference between the zonal wavenumber 1 and 2 contributions to the anomalous circulation and the climatological stationary eddy field in the troposphere. They showed that constructive interference coincides with greater vertical propagation of planetary-scale wave activity and a deceleration of the stratospheric polar vortex. Opposite behaviour was found for destructive interference, which is associated with weaker vertical planetary-scale wave activity propagation and a strengthening of the stratospheric polar vortex.

To examine if there are large differences in the vertical propagation of wave activity into the stratosphere between the various NAO events, we calculate the zonal-mean meridional heat flux, i.e., the vertical component of the Eliassen-Palm flux vector, from 30°N to the North Pole, for zonal wave numbers 1 and 2, averaged from 100 hPa to 70 hPa (Fig. 9). For the NAO-|MJO events (Fig. 9a), consistent with the negative NAM index in the stratosphere (Fig. 8a), we see a strengthening of the vertical propagation of planetary-scale wave activity into the stratosphere at all lags after lag -50 days, except for a brief period centred near lag -5 days. For the NAO-|nMJO events (Fig. 9b), the meridional heat flux undergoes several sign changes, with values being smaller than those for the NAO-|MJO events. A comparison with the NAM index in the stratosphere (Fig. 8b) shows a consistent relationship between the sign changes in the meridional heat flux, and the strengthening and weakening of the stratospheric polar vortex.

For the NAO+|MJO events (Fig. 9c), consistent with the positive stratospheric NAM index (Fig. 8c), we see a weakening of the vertical propagation of planetary-scale wave activity into the stratosphere at all lags after lag -50 days, excepted for brief intervals centred near lag -25 and lag -10 days. For the NAO+|nMJO events (Fig. 9d), as with the NAO-|nMJO events, a number of sign changes in the meridional heat fluxes are observed that are consistent with the fluctuations seen in the strength of the stratospheric polar vortex (Fig. 8d).

To gain further insight into the relationship between the stratosphere and the NAO|MJO and the NAO|nMJO events, we examine lagged composites of the anomalous 70-hPa streamfunction field. For the NAO-|MJO events (Fig. 10a), a steadily amplifying zonally symmetric anomalous circulation in the lower stratosphere is seen. This contrasts with the NAO-|nMJO events, which are overshadowed by zonal wavenumber 2 (Fig. 10b). The NAO+|MJO events show similar features but with opposite sign, as the anomalous 70-hPa streamfunction field for the NAO+|MJO events is also dominated by its zonally symmetric component (Fig. 10c) and the NAO+|nMJO events by its zonal wavenumber 2 contribution (Fig. 10d). These findings show that when the MJO is active and the NAM index in the lower stratosphere is large (Figs. 8a and 8c), the changes in the flow are primarily associated with the zonally-symmetric component of the flow. When the MJO is inactive, the zonal mean flow changes in the lower stratosphere are relatively small. Together with the results shown in Fig. 9 for the planetary-scale vertical wave activity propagation, these results suggest that NAO/MJO events are preceded by strong wave/zonal mean flow interaction in the lower stratosphere, whereas those NAO events that are unrelated to the MJO show little wave/zonal mean flow interaction in the stratosphere. For the NAO/MJO events, the large amplitude zonally-symmetric 70-hPa streamfunction anomalies are associated with a NAM signature at the surface, which most likely occurs via downward control and eddy feedback, as has been shown in

many studies (e.g., Polvani and Kushner, 2002; Kushner and Polvani, 2004; Song and Robinson, 2004; Simpson et al., 2009). In contrast, when the MJO is not active, it appears that a local NAO (Figs. 6b and 7b) confined to the North Atlantic takes place with limited influence from the stratosphere.

5. Conclusions

In this study, we investigated the relationship between the MJO and the NAO. The approach adopted was to divide NAO events into two categories, one preceded by an active MJO and the other by the absence of an active MJO, and then to examine the relationship with stratospheric polar vortex. The general picture can be summarized as follows, where the symbol → denotes the transition from one phenomenon to the next. All relationships shown involve statistically significant ($p<0.10$) anomalies.

NAO-|MJO: eastward propagating MJO convection from the Maritime Continent to the tropical western and central Pacific → long-lived (about 30 days) NAM- throughout both the troposphere and stratosphere

NAO-|nMJO: a localized and relatively short-lived (about 10 days) NAO- develops that is limited to the troposphere over the North Atlantic

NAO+|MJO: eastward propagating MJO convection from the western tropical Indian Ocean to the Maritime Continent → long-lived (about 30 days) NAM+ throughout both the troposphere and stratosphere

NAO+|nMJO: a localized and relatively short-lived (about 10 days) NAO+ forms that is confined to the troposphere over the North Atlantic

In other words, when the MJO is active, both phases of the NAO are associated with a midlatitude SLP anomaly over the North Pacific at the same latitude and with the same sign as that over the North Atlantic. In this sense, when the MJO is active, the NAO is more accurately described by the NAM. In contrast, when the MJO is not active, a SLP anomaly over the North Pacific of the same sign as that over the North Atlantic is not present. In this case, the localized NAO dipole pattern develops.

The sensitivity of the above steps to the particular NAO index was examined by performing an EOF analysis with the 300-hPa geopotential height NAO in a manner that was identical to that for our SLP NAO index. We examined the sensitivity of the main results of our study to the 300-hPa geopotential height NAO index. For the RMM1 and RMM2 indices, it was found that the timing and amplitude of the statistically significant RMM1 and RMM2 anomalies are rather similar to those for the SLP NAO index (not shown). For the Baldwin and Dunkerton (1999) stratospheric NAM indices, at negative lags, statistically significant anomalies were found to extend to 70 hPa for the NAO-|MJO (beginning at lag -20 days) and 10 hPa for the NAO+|MJO (beginning at lag -40 days) (not shown). The presence of stratospheric NAM anomalies at negative lags compares well with the corresponding anomalies in Fig. 8, except that the anomalies at negative lags do not extend as high

into the stratosphere for the 300-hPa geopotential height NAO index. Furthermore, for the 300-hPa geopotential height NAO-|nMJO and NAO+|nMJO events, as in Fig. 8 at negative lags, the anomalies are mostly confined to the troposphere (not shown). These results suggest that the key results of our study are not overly sensitive to the type of NAO index being used.

What accounts for the difference in the above spatial characteristics between the NAO|MJO, or equivalently the NAM, and the localized NAO|nMJO? Our findings suggest that the key may be the influence of the stratospheric polar vortex. The NAO|MJO events are preceded by either an increase (for the NAO-|MJO) or decrease (for the NAO+|MJO) in the vertical propagation of planetary-scale wave activity into the stratosphere. For the NAO-|MJO events, this is followed by a weakening of the zonally-symmetric component of the lower stratospheric zonal wind, and then by the excitation of the annular-like NAM-, and vice versa for the NAO+|MJO events. In contrast, for the NAO|nMJO events, the planetary-scale wave activity propagation from the troposphere into the stratosphere is weaker and less persistent, resulting in little change to the zonally-symmetric component of the lower stratospheric zonal wind. As a result, a much more localized NAO dipole anomaly develops, rather than the NAM with its annular-like structure.

It is worth noting that in spite of these differences between the NAO|MJO and NAO|nMJO events, for all of the NAO events, the impact of the eddy vorticity fluxes

was found to resemble that obtained in previous studies (Lorenz and Hartmann, 2001; Feldstein, 2003; Benedict et al., 2004). By projecting the composite inverse Laplacian of the 300-hPa transient eddy vorticity flux divergence onto the composite anomalous 300-hPa streamfunction field when the NAO index attains its maximum amplitude (Feldstein, 2003), it was found that the low-frequency (greater than 10 days) transient eddy vorticity flux contributes to the growth and the decay of the NAO, whereas the high-frequency (less than 10 days) transient eddy vorticity flux contributes to the NAO growth and maintenance (not shown).

One point that was not addressed in the study is the question of what process triggers the NAO events when the MJO is inactive. In the modelling study of Franzke et al. (2004), it was found that synoptic-scale disturbances propagate eastward from the North Pacific to the North Atlantic where wave breaking results in the formation of both NAO phases. In that study, the development of the NAO involved dynamical processes that are confined to the midlatitude troposphere. It is plausible that NAO|nMJO events in the atmosphere may also be triggered by a similar midlatitude process.

Acknowledgements

Most of the research for this manuscript was performed when the first author visited the Pennsylvania State University. We thank the Pennsylvania State University

for offering very good working conditions. We also thank the European Centre for Medium-Range Weather Forecasts for providing us with the ERA-Interim reanalysis data. We also thank two anonymous reviewers for their helpful comments. This work is jointly supported by the National Natural Science Foundation of China (Grant 41230420), the National Key Basic Research and Development (973) Project (Grant 2012CB417204), National Science Foundation grants AGS-1036858, AGS-1401220, and AGS-1139970, and National Oceanic and Atmospheric Administration grant NA14OAR4310190.

References

Baldwin MP, and Dunkerton TJ. 1999. Propagation of the Arctic Oscillation from the stratosphere to the troposphere. *J. Geophysical Research* 104: 30937-30946.

Baldwin MP, and Dunkerton TJ. 2001. Stratospheric harbingers of anomalous weather regimes. *Science* 294: 581-584.

Benedict JJ, Lee S, and Feldstein SB. 2004. Synoptic view of the North Atlantic Oscillation. *J. Atmos. Sci.* 61: 121-144.

Cassou C. 2008. Intraseasonal interaction between the Madden-Julian Oscillation and the North Atlantic Oscillation. *Nature* 455: 523-527.

Dee DP, Uppala SM, Simmons AJ, and coauthors. 2011. The ERA-Interim reanalysis: configuration and performance of the data assimilation system. *Quart. J. Roy.*

Meteor.Soc. 137: 553–597.

DeWeaver E, and Nigam S. 2000. Do stationary waves drive the zonal-mean jet anomalies of the northern winter? *J. Climate* 13: 2160 – 2176.

Franzke C, Lee S, and Feldstein SB. 2004. Is the North Atlantic Oscillation a breaking wave? *J. Atmos. Sci.* 61: 145-160.

Feldstein SB. 2000. Teleconnections and ENSO: The timescale, power spectra, and climate noise properties. *J. Climate* 13: 4430-4440.

Feldstein SB. 2003. The dynamics of NAO teleconnection pattern growth and decay. *Quart. J. Roy. Meteorl. Soc.* 129: 901-924.

Feldstein SB, and Franzke C. 2006. Are the North Atlantic Oscillation and the Northern Annular Mode distinguishable? *J. Atmos. Sci.* 63: 2915-2930.

Feldstein SB, and Lee S. 1996. Mechanisms of zonal index variability in an aquaplanet GCM. *J. Atmos. Sci.* 53: 3541-3555.

Garfinkel CI, Hartmann DL, and Sassi F. 2010. Tropical precursors of anomalous Northern Hemisphere stratospheric polar vortices. *J. Climate* 23: 3282-3299.

Garfinkel CI, Feldstein SB, Waugh DW, Yoo C, and Lee S. 2012. Observed connection between stratospheric sudden warmings and the Madden-Julian Oscillation. *Geophys. Res. Lett.* 39: L18807, doi:10.1029/2012GL053144.

Garfinkel CI, Waugh DW, Gerber EP. 2013. The effect of tropospheric jet latitude on coupling between the stratospheric polar vortex and the troposphere. *J. Climate* 26:

2077-2095.

Gerber EP, Baldwin MP, Akiyoshi H, and coauthors. 2010. Stratosphere-Troposphere coupling and Annular Mode variability in chemistry-climate models. *J. Geophys. Res.* 115: D00M06, doi:10.1029/2009JD013770.

Hurrell JW. 1995. Decadal trends in the North Atlantic Oscillation regional temperatures and precipitation. *Science* 269: 676–679.

Hurrell JW, and Loon HV. 1997. Decadal variations associated with the North Atlantic Oscillation. *Climatic Change* 36: 301-326.

Jiang ZN, Mu M, and Luo DH. 2013. A study of the North Atlantic Oscillation using conditional nonlinear optimal perturbation. *J. Atmos. Sci.* 70: 855-875.

Kushner PJ, and Polvani LM. 2004. Stratosphere-troposphere coupling in a relatively simple AGCM: The role of eddies. *J. Climate* 17: 629-639.

Lee S, and Feldstein SB. 1996. Mechanism of zonal index evolution in a two-layer model. *J. Atmos. Sci.* 53: 2232-2246.

Lee S, and Kim HK. 2003. The dynamical relationship between subtropical and eddy-driven jets. *J. Atmos. Sci.* 60: 1490-1503.

Liebmann B, and Smith CA. 1996. Description of a complete (interpolated) outgoing longwave radiation dataset. *Bull. Amer. Meteor. Soc.* 77: 1275-1277.

Lin H, Brunet G, and Derome J. 2009. An observed connection between the North Atlantic Oscillation and the Madden-Julian Oscillation. *J. Climate* 22: 364-380.

Lin H, Brunet G, and Fontecilla JS. 2010. Impact of the Madden–Julian Oscillation on the intraseasonal forecast skill of the North Atlantic Oscillation. *Geophys. Res. Lett.* 37: doi:10.1029/ 2010GL044315.

Lorenz DJ, and Hartmann DL. 2001. Eddy-zonal flow feedback in the Southern Hemisphere. *J. Atmos. Sci.* 58: 3312-3327.

Lorenz DJ, and Hartmann DL. 2003. Eddy-zonal feedback in the Northern Hemisphere winter. *J. Climate* 16: 1212-1227.

Luo DH, Lupo A, and Wan H. 2007. Dynamics of eddy-driven low-frequency dipole modes. Part Ⅰ: A simple model of North Atlantic Oscillations. *J. Atmos. Sci.* 64: 3-28.

Madden RA, and Julian PR. 1971. Detection of a 40–50 day oscillation in the zonal wind. *J. Atmos. Sci.* 28: 702–708.

Madden RA, and Julian PR. 1994. Observations of the 40–50 day tropical oscillation—A review. *Mon. Wea. Rev.* 122: 814–837.

Polvani LM, and Kushner PJ. 2002. Tropospheric response to stratospheric perturbations in a relatively simple general circulation model. *Geophys. Res. Lett.* 29: doi:10.129/2001GL014284.

Riddle EE, Stoner MB, Johnson NC, L'Heureux ML, Collins DC, and Feldstein SB. 2013. The impact of the MJO on clusters of wintertime circulation anomalies over the North American region. *Clim. Dyn.* 40: 1749-1766.

Robinson WA. 1991. The dynamics of the zonal index in a simple model of the atmosphere. *Tellus A* 43: 295–305. doi: 10.1034/j.1600-0870.1991.t01-4-00005.x

Rossby CG. 1939. Relation between variations in the intensity of the zonal circulation of the atmosphere and the displacements of the semi-permanent centers of action. *J. Mar. Res.* 2: 38-55.

Simpson IR, Blackburn M, and Haigh JD. 2009. The role of eddies in driving the tropospheric response to stratospheric heating perturbations. *J. Atmos. Sci.* 66: 1347-1365.

Smith KL, Kushner PJ, and Cohen J. 2011. The role of linear interference in northern annular mode variability associated with Eurasian snow cover extent. *J. Climate* 24: 6185-6202.

Song Y, and Robinson WA. 2004. Dynamical mechanisms for stratospheric influences on the troposphere. *J. Atmos. Sci.* 61: 1711-1725.

Thompson DWJ, and Wallace JM. 1998. The Arctic Oscillation signature in the wintertime geopotential height temperature fields. *Geophys. Res. Lett.* 25: 1297-1300.

Thompson DWJ, and Wallace JM. 2000. Annular modes in the extratropical circulation. Part I: month-to-month variability. *J. Climate* 13: 1000–1016.

Vallis GK, Gerber EP, Kushner PJ, and Cash BA. 2004. A mechanism and simple dynamical model of the North Atlantic Oscillation and annular modes. *J. Atmos. Sci.* 61: 269-280.

Vitart F, and Molteni F. 2010. Simulation of the Madden-Julian oscillation and its teleconnections in the ECMWF forecast system. *Quart. J. Roy. Meteor. Soc.* 136: 842-855.

Walker GT, and Bliss EW. 1932. World Weather V. *Mem. Roy.Meor. Soc.* 4: 53–83.

Wheeler MC, and Hendon HH. 2004. An all-season real-time multivariate MJO index: Development of an index for monitoring and prediction. *Mon. Wea. Rev.* 132: 1917-1932.

Yu JY, and Hartmann DL. 1993. Zonal flow vacillation and eddy forcing in a simple GCM of the atmosphere. *J. Atmos. Sci.* 50: 3244-3259.

Zhou S, and Miller AJ. 2005. The interaction of the Madden–Julian oscillation and the Arctic Oscillation. *J. Climate* 18: 143–159.

Figure Captions

Figure 1: The first empirical orthogonal function of the sea level pressure field confined to the North Atlantic between 25°N and 80°N and between 70°W and 40°E. Solid contours are positive, dashed contours negative, and the zero contour is omitted.

Figure 2: The lagged composite NAO indices for (a) the NAO- events; and (b) the NAO+ events. The dots indicate statistically significance above the 90% confidence level according to a two-sided Student's *t*-test.

Figure 3: The composites of RMM1, RMM2, and the MJO amplitude for (a) the NAO-|MJO events; (b) the NAO-|nMJO events; (c) the NAO+|MJO events, and (d) the NAO+|nMJO events. The dots indicate statistically significance above the 90% confidence level according to a two-sided Student's *t*-test.

Figure 4: The DJF composite OLR and 850-hPa wind vector anomalies. Shading levels indicate OLR anomalies less than -7.5, -15, -22.5, and -30 W m^{-2}, respectively, and hatching levels denote OLR anomalies greater than 7.5, 15, and 22.5 W m^{-2}, respectively. [Adapted from Wheeler and Hendon (2004).]

Figure 5: The composite anomalous outgoing long wave radiation for (a) the NAO-|MJO events; (b) the NAO-|nMJO events; (c) the NAO+|MJO events, and (d) the NAO+|nMJO events (The contour interval is 4). The shaded areas indicate statistically significance above the 90% confidence level according to a two-sided

Student's *t*-test.

Figure 6: The evolution of the composite anomalous sea level pressure field for (a) the NAO-|MJO events, and (b) the NAO-|nMJO events (contour interval is 2 hPa). The bottom panels show the time average between lag -10 and lag +10 days (contour interval is 1 hPa). Solid contours are positive, dashed contours negative, and the zero contour is omitted. The shaded areas indicate statistically significance above the 90% confidence level according to a two-sided Monte Carlo bootstrapping test.

Figure 7: As Fig. 6, except for (a) the NAO+|MJO events, and (b) the NAO+|nMJO events.

Figure 8: The lagged composite NAM indices for (a) the NAO-|MJO events, (b) the NAO-|nMJO events, (c) the NAO+|MJO events, and (d) the NAO+|nMJO events (contour interval is 0.2). The shaded areas correspond to statistically significance above the 90% confidence level for a two-sided Student's *t*-test.

Figure 9: The vertical component of the Eliassen-Palm flux vector, from 30°N to the North Pole, for zonal wave numbers 1 and 2, averaged from 100 hPa to 70 hPa, for (a) NAO-|MJO events, (b) the NAO-|nMJO events, (c) the NAO+|MJO events, and (d) the NAO+|nMJO events. The shaded areas correspond to statistically significance above the 90% confidence level for a two-sided Student's *t*-test.

Fig. 10 The lagged composite anomalous 70-hPa streamfunction field for (a) the NAO-|MJO events, (b) the NAO-|nMJO events, (c) the NAO+|MJO events, and (d)

the NAO+|nMJO events (contour interval is 300 $m^2 s^{-1}$). Solid contours are positive, dashed contours negative, and the zero contour is omitted. The shaded areas indicate statistically significance above the 90% confidence level according to a two-sided Monte Carlo bootstrapping test.

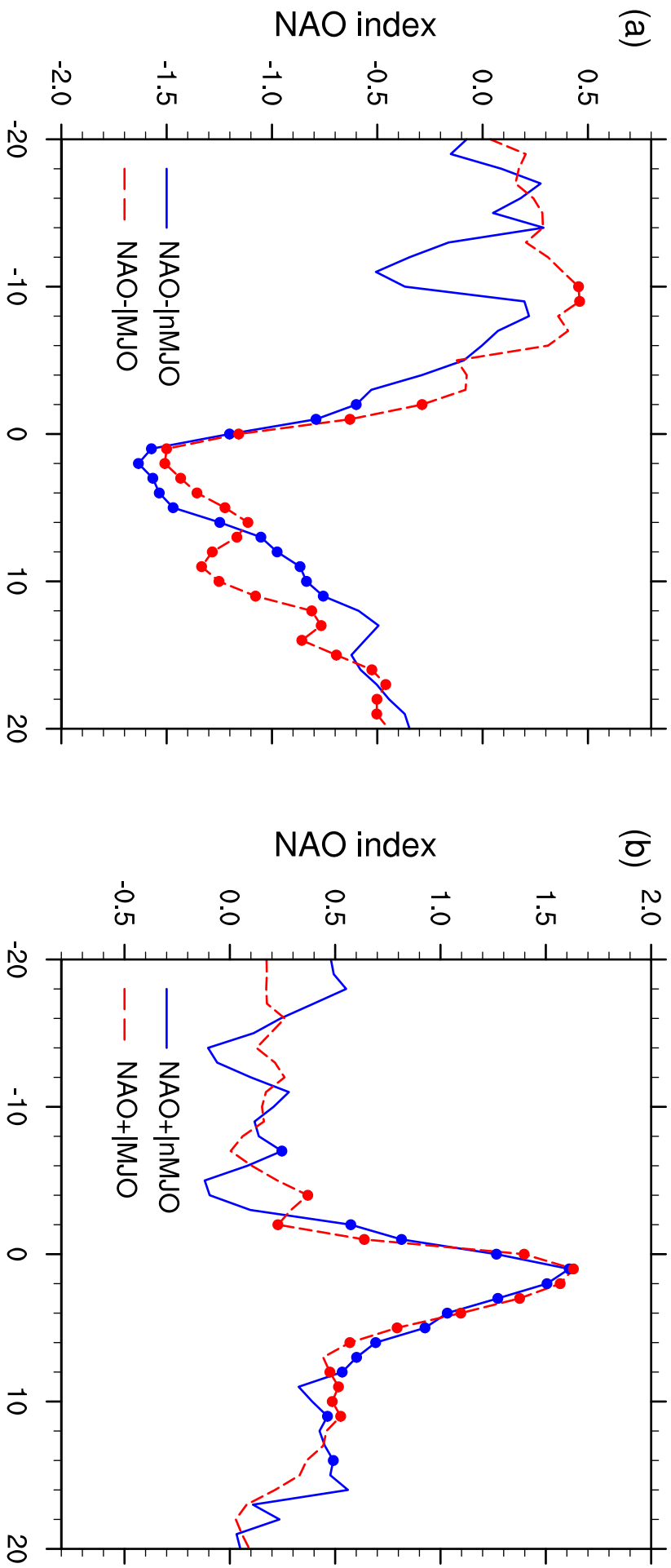

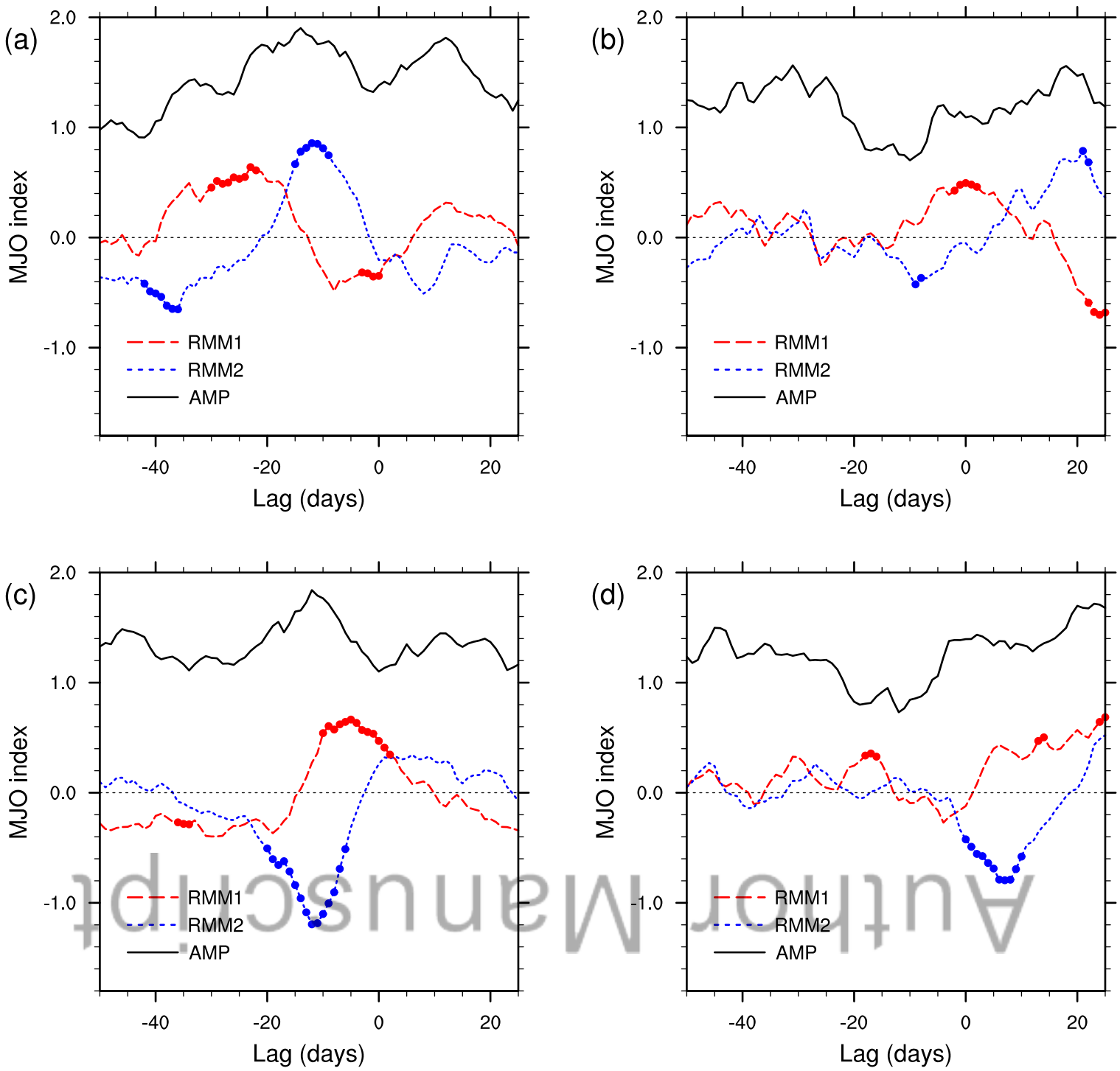

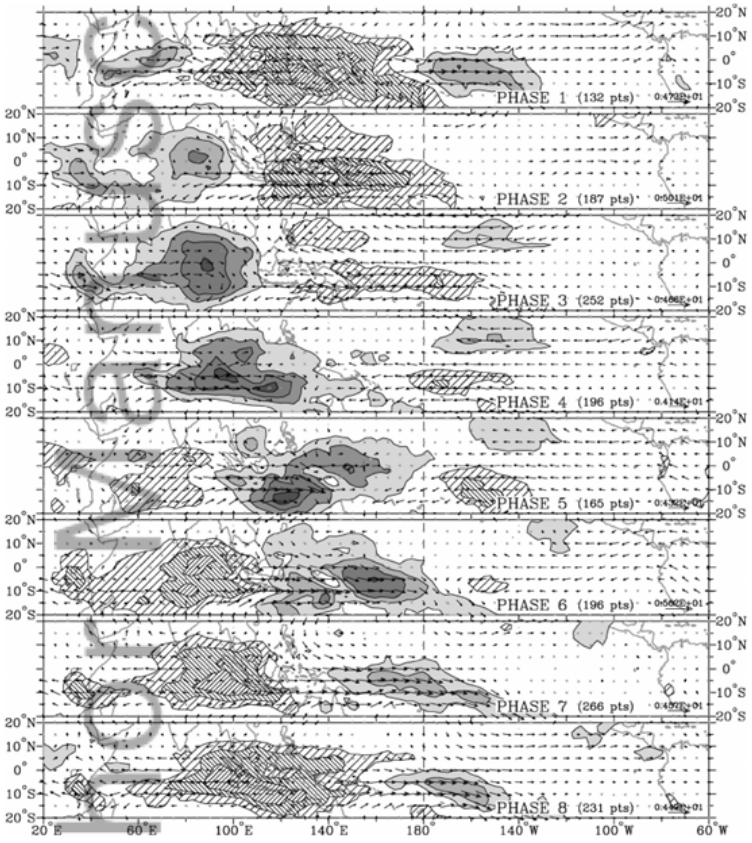

fig4.WH2004.tif